Biosensors

DOI: 10.1002/anie.201205346

Continuous Evolution Profiles for Electronic-Tongue-Based Analysis**

Yanxia Hou, Maria Genua, Dayane Tada Batista, Roberto Calemczuk, Arnaud Buhot, Pauline Fornarelli, Jamal Koubachi, David Bonnaffé,* Els Saesen, Cédric Laguri, Hugues Lortat-Jacob, and Thierry Livache**

Conventional biosensors and biochips rely on a "lock-and-key" recognition principle, for which specific ligands, such as aptamers, antibodies, or mimetics are needed. In contrast, electronic nose/tongue devices (eN/eT)[1–10] use the differential binding of analytes, either alone or in mixtures, to an array of cross-reactive receptors (CRRs) whose combined responses create a characteristic pattern for each component.[11] As a result, none of the CRRs need to be highly specific for any given analyte and the time-consuming design and generation of specific sensors may be circumvented.[12] Based on this principle, CRR arrays associated with appropriate detection have been developed.[13,14] For example, synthetic tetraphenylporphyrin derivatives, whose fluorescence quenching upon protein binding was used for detection, or a receptor library, integrating a peptide cavity coupled with indicator-uptake colorimetric detection, were developed for protein sensing above concentrations of ten micromolar.[15–17] A sensor array composed of gold nanoparticles, grafted with different amino-functionalized thiols and conjugated with an anionic fluorescent polymer (poly(*p*-phenyleneethynylene, PPE), allowed detection of proteins in the low nanomolar range, as well as detection of bacteria[19] or discrimination of normal cells from their cancerous counterparts.[18–20] Furthermore, replacing PPE with green fluorescent protein led to a concentration-sensitive CRR array able to discriminate different proteins in human serum at physiologically relevant concentrations.[21]

However, though simplified with regard to conventional biosensors, the preparation of eN/eT sensing arrays still requires the design and synthesis 5–29 CRRs and conjugation to a ligand-independent detection system. The development of new eN/eT applications would thus benefit from simplified production of the sensing elements. In this regard, eN applications take advantage of the differential diffusion of volatile biomarkers through films of a single sensing material in varying morphology and surface coverage.[9] For an eT, we anticipated that the design and synthetic efforts could also be drastically reduced if the CRRs were prepared by self-assembly of different combinations of building blocks (BBs), that is easily accessible molecules displaying different physicochemical properties. In this way, simply mixing different BBs in varying and controlled proportions and allowing them to assemble, either alone or on a template, should lead to a collection of combinatorial cross-reactive receptors (CoCRRs) with evolutionary properties. Interestingly, a high diversity of CoCRRs can be produced from a restricted number of BBs: 11 with only two BBs mixed in concentrations varying from 0 to 100% in 10% increments and 66 by simply adding a third BB. Further generalization to n BBs and i% concentration increment leads to $[(100/i)+n-1]!/[(n-1)!(100/i)!]$ potential different CoCRRs. To assure 1) reproducible assembly; 2) close correlation between the CoCRRs topology and the precursor combination of BBs; 3) spatial encoding of the CoCRRs compositions, we reasoned that the BBs would best be combined through the formation of self-assembled monolayers (SAMs). Interestingly, if the gold surface of a surface plasmon resonance imaging (SPRi)[22] prism was used for the formation of SAMs through thiol or disulfide bonds,[23] a label-free, synchronous, parallel, and real-time observation of binding events on the CoCRRs array could also be performed (Figure 1).

To investigate this hypothesis, we designed a model array inspired by the way cell-surface heparan sulfates (HS) recognize HS binding proteins (HSbps), an important group of extracellular mediators involved in many physiological and pathological processes.[24,25] HS are negatively charged polysaccharides displaying a high degree of molecular diversity, which arises from the regulated generation of various epimerization and sulfation patterns during biosynthesis. According to cell type and activation state, HS chains with different negatively charged topologies are expressed, presumably to promote selective interactions with HSbps.[26,27]

[*] Dr. Y. Hou, M. Genua, Dr. D. Tada Batista, Dr. R. Calemczuk, Dr. A. Buhot, Dr. T. Livache
SPrAM, UMR 5819 (CEA-CNRS-UJF-Grenoble 1), INAC/CEA-Grenoble
38054 Grenoble cedex 9 (France)
E-mail: yanxia.hou-broutin@cea.fr
thierry.livache@cea.fr

P. Fornarelli, Dr. J. Koubachi, Prof. D. Bonnaffé
ICMMO/G2M/LCOM, UMR 8182 (CNRS-UPS), LabEx LERMIT, Université Paris-Sud
91405 Orsay cedex (France)
E-mail: david.bonnaffe@u-psud.fr

E. Saesen, Dr. C. Laguri, Dr. H. Lortat-Jacob
Institut de Biologie Structurale, SAGAG, UMR 5075 (CEA-CNRS-UJF-Grenoble 1)
38027 Grenoble cedex 01 (France)

[**] This work has been financially supported by the French National Research Agency (ANR-grant 06-NANO-045).

Supporting information for this article (experimental details) is available on the WWW under http://dx.doi.org/10.1002/anie.201205346.

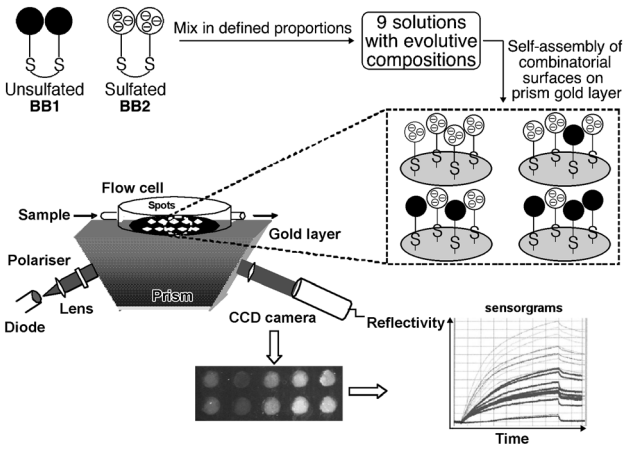

Figure 1. Illustration of a novel electronic tongue composed of an array of combinatorial cross-reactive receptors, obtained by self-assembly of mixtures of building blocks **BB1** and **BB2** spotted on the gold surface of an SPRi prism, allowing protein detection by SPR imaging.

We hypothesized that a first "proof of principle" CoCRRs array able to differentiate HSbps could be prepared from **BB1** and **BB2**, both easily derived from β-allyl lactoside[28] (Figure 1 and 2). These BBs are both hydrophilic but **BB1** is neutral while **BB2** is highly negatively charged. We anticipated that variation of the **BB2** to **BB1** ratio in the spotted solutions should provide, following self-assembly, CoCRRs displaying different charge densities that could bind three distinct HSbps with different affinities: the α and γ isoforms of the chemokine CXCL12[29] along with the pro-inflammatory cytokine interferon-γ (IFNγ).[30] *Erythrina cristagalli* lectin (ECL), a non-HSbp, was added to this set as a negative control for binding on CoCRRs containing high ratio of **BB2**. In addition, ECL is documented to bind lactose[31] and should thus provide a positive reference for the CoCRRs rich in **BB1**.

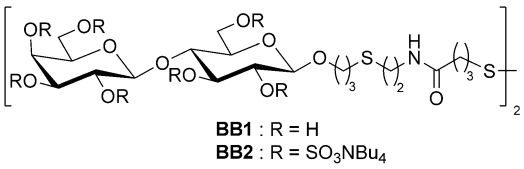

Figure 2. Formulas of the two disulfide building blocks **BB1** and **BB2** used to construct the combinatorial cross-reactive receptors array.

Using **BB1** and **BB2**, at a constant total concentration of 20 μM, we prepared nine mixtures with [**BB1**]/([**BB1**]+[**BB2**]) ratios of 0, 10, 20, 30, 50, 70, 80, 90, and 100%. These mixtures were then spotted on the gold surface of an SPRi prism and incubated overnight to generate an array of nine CoCRRs by self-assembly. For each spot, the ratio of the two BBs anchored on the gold surface was assumed to be equal to the molar ratio in the parent solution.[32,33] Importantly, the SPR signals measured from the nine spots upon infusion of buffer in the absence of protein were independent of the BB, demonstrating a similar overall coverage of the gold film for all CoCRRs (see Section 4 of the Supporting Information). An initial challenge of the system for protein detection was performed by injecting ECL solutions at different concentrations (200, 400, 800 nM, and 1.6 μM). As expected, the spots showed different levels of response, the images were recorded and subsequently converted to a series of sensorgrams. The reflectivities at the end of the ECL injection on CoCRRs at different concentrations were used to establish a calibration curve that exhibits a Langmuir adsorption profile (Supporting Information, Figure S4), confirming the capacity of our system to function as a detection array.

Then, to probe the ability of the CoCRRs array to differentiate HSbps from non-HSbp analytes, we sequentially injected solutions of ECL (200 nM), CXCL12α (100 nM), CXCL12γ (100 nM), and IFNγ (25 nM). Analysis of the sensorgrams (not shown) revealed that, for each protein, the different CoCRRs displayed different reflectivities. More importantly, the individual response of each protein on a given CoCRR is dependent on the composition of the parent BB mixture. In other words, for a given CoCRR composition, the intensity of the response is dependent on the protein injected, indicating that the CoCRRs array responds differently toward each protein, as illustrated in Figure 3.

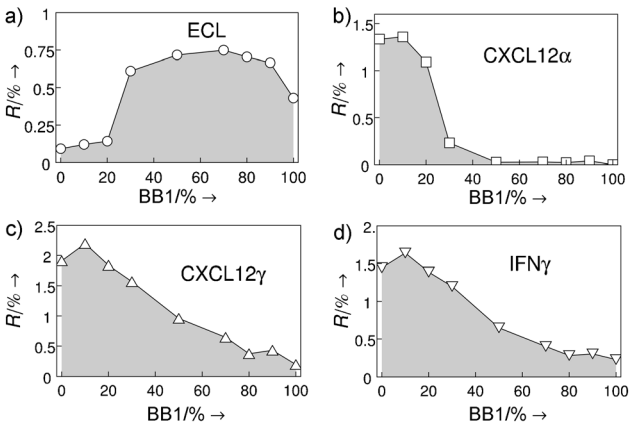

Figure 3. Continuous evolution profiles (CEP) obtained from the CoCRRs array for proteins a) ECL (200 nM), b) CXCL12α (100 nM), c) CXCL12γ (100 nM) and d) IFNγ (25 nM). The recognition patterns were generated by plotting the reflectivity (*R*) at the end of injection versus the [**BB1**]/([**BB1**]+[**BB2**]) ratio.

These results could be considered sufficient to establish the **BB1**-**BB2** CoCRRs arrays coupled to SPRi detection as an efficient eT. But the data presented in Figure 3, illustrate an original and advantageous behavior of the CoCRRs-array approach. The response obtained from a given CoCRR for a given protein is not a simple linear addition of the responses obtained on the pure **BB1** and **BB2** spots. This non-linear behavior allows each combinatorial receptor to generate additional information relative to its neighbors, which justifies the use of a set of CoCRRs instead of spots of pure **BB1** or **BB2**. In addition, since the array design and construction allow the composition of each CoCRR to be linked and close to the ones of its neighbors, each receptor delivers a signal that is related to that of its neighbor. Therefore, the data

generated by the CoCRRs array can be considered as continuous and, for each protein, a recognition pattern with a continuous evolution profile (CEP) can be interpolated. This behavior is in striking contrast with the sets of uncorrelated discrete data obtained with traditional eN/eT approaches; with the CoCRRs array, the signal of one receptor correlates with the others and abnormal signals arising from a defective one can be identified and excluded. This characteristic can be compared to the ability of our brain to reconstruct an image from a screen, even when defective pixels are present. Furthermore, injection of each protein at different concentrations demonstrated that, even though the intensity of the signals varied according to the concentration, the shape of the CEP remained unchanged. Therefore, in principle, the CEP shape can be used to identify proteins in large range of concentrations.

We further explored whether the CEP obtained for each protein could be used for reliable identification. As shown in Figure 3, ECL can easily be differentiated from HSbps. The CEP of ECL, reaching a maximum for the CoCRR containing 70% of **BB1**, is completely different from the ones obtained for the three HSbps that display maximal signals at 10% **BB1**. As expected, ECL shows a higher affinity for CoCRRs rich in **BB1**, while HSbps have higher affinity for CoCRRs with a higher content of sulfated **BB2**. At this level of discrimination, two CRRs of pure **BB1** and **BB2** would have been sufficient to differentiate ECL from HSbps. However, the advantage of enhancing the receptor diversity by combining BBs is evidenced by the comparison of the CEP obtained for the HSbps (Figure 3). These three proteins display similar behavior towards pure **BB1** or **BB2** receptors, but they differ notably in their binding to receptors of mixed compositions. The reflectivity of CXCL12α is almost zero when the **BB1** content in the CoCRR is 50% or higher, whereas CXCL12γ and IFNγ still bind significantly on CoCRR containing up to 70% **BB1**. Unfortunately, the CEP of IFNγ is barely distinguishable from the one of CXCL12γ. It may seem paradoxical that the two CXCL12 isoforms showed better discrimination than CXCL12γ from IFNγ. However, we believe that such behavior reveals a unique and advantageous feature of the **BB1**-**BB2** CoCRRs array for the analysis of HSbps. Indeed, both CXCL12 isoforms share the same first 68 amino acid residues, are similarly folded, and display a typical HS binding site (K24-K27-R41) located in a highly structured domain. However, CXCL12γ possesses an additional unfolded C-terminal extension with an additional HS binding site.[29] Similarly IFNγ, a C_2 symmetric homodimer in solution, folds into a rigid core, flanked by the C-terminal regions of each subunit that contain two clusters of basic residues displaying a high conformational flexibility.[30] Thus, both CXCL12γ and IFNγ possess two distant HS binding domains, with at least one of them being located in an unfolded part of the protein whose flexibility could maximize contact points with their ligands at low energetic cost through conformational fluctuations.[34] In contrast, the single CXCL12α HS binding domain is located in a rigid domain that may limit the adaption of the conformations of basic residues to low charge density CoCRRs. Taken together, these results reveal that the **BB1**-**BB2** CoCRRs array is very sensitive to the charge topologies of HSbps and the approach we describe herein offers an unprecedented and simple tool to investigate the overall organization of the HS domains (charge density and distribution along the chain), independent of the fine structure found in the polymer (specific sulfation and epimerization sequences).[35,36]

Beyond the detection and identification of pure analytes, a long-term goal of the eN/eT technology is to analyze complex mixtures. We thus decided to challenge the nine **BB1**-**BB2** CoCRRs array with protein mixtures. Mix1 (200 nM ECL and 100 nM CXCL12α) was thus injected onto the array, and a simple visual examination of the resulting CEP established that the CoCRRs array was able to discriminate between Mix1 and the individual proteins (Figure 4A). Moreover, the Mix1 CEP shows additive behavior with respect to the signals obtained from the pure proteins. An identical behavior was also observed with Mix2 (100 nM CXCL12α and 25 nM IFNγ) and Mix3 (200 nM ECL and 25 nM IFNγ), confirming the ability of the CoCRRs sensing/CEP analysis for the identification of components in mixtures by a simple linear decomposition of the CEP into the pure analytes.

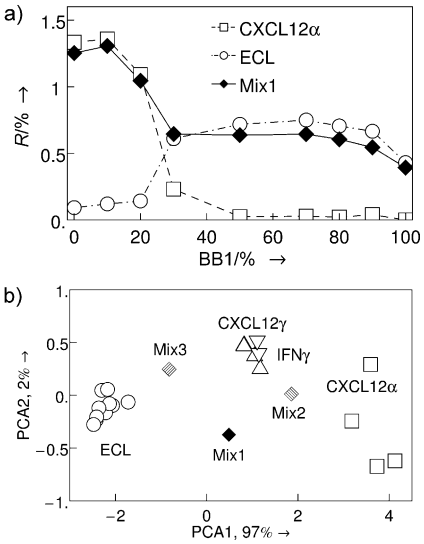

Figure 4. a) CEP of Mix1 (ECL + CXCL12α; ◆) compared to the ones of pure ECL (○) and CXCL12α (□); b) Two-dimensional PCA score plot showing clustering of the four proteins and the three mixtures for differentiation. The multiple dots for a given protein correspond to different concentrations.

Acquisition of the data described above was performed over a period of six months on different batches of the 9-CoCRRs arrays, and each array was in continuous use for at least two weeks with more than 20 protein injection/regeneration cycles. In addition, after storage for four months at 4 °C, the same system could be reused without alteration of the acquired data. However, after six months of storage at 4 °C, the array functioned significantly worse. Taken together, these data showed a good correlation (> 98%) between different full CEP patterns from measurement to measure-

ment (see Part 7 of the Supporting Information) and more than 93% correlation from batch to batch (Figure S5).

Because visual examination of the CEPs is prone to subjective interpretation, all CEP patterns were analyzed using principal component analysis (PCA) to give an objective result. The resulting two-dimensional PCA score plot (Figure 4B) established that the first two components represent more than 99% of the variability of the data set. In this figure, the different dots for a given protein correspond to experiments performed at various concentrations. Clustering of the analytes illustrates the ability of the **BB1**-**BB2** CoCRRs array to discriminate between the pure as well as mixed protein samples. Indeed, ECL is clearly distinguishable from the other proteins, while CXCL12α isoform is readily distinguished from the other HSbps. As expected, the clustering patterns of CXCL12γ and IFNγ are mostly overlapping, indicating that the PCA analysis did not allow for their differentiation. The CEP patterns of the protein mixtures Mix1–Mix3 were also analyzed with PCA. Their corresponding dots lie in between the clusters of the pure proteins, confirming that the interactions of the proteins in the mixtures with the array are additive.

As shown above, the CEP pattern analysis brings more reliable information than the signals of non-correlated CRRs obtained from previously described eN/eT studies. In principle, the acquisition of such correlated data sets is not restricted to SPRi detection. However, one of the main advantages of SPRi is the ability to monitor the real-time adsorption and desorption kinetics, introducing a new discrimination parameter. Indeed, two analytes presenting the same relative affinity for a set of CoCRRs may differ in their kinetics of interaction. In Figure 5, the time-dependent recognition patterns for ECL and CXCL12α are displayed. Such continuous evolution landscapes (CELs), where time is added to the two-dimensional CEP analysis, illustrate the added value of real-time SPRi interaction measurements. Simple visual examination reveals that desorption of ECL is much faster than that of CXCL12α. Consequently, discrimination between the two proteins by the 3D CEL patterns is more straightforward relative to 2D CEP. The third CEL, corresponding to the infusion of Mix1, shows that the CEL follows the additive behavior found for CEPs. Such kinetic information should facilitate the future identification of analytes in a mixture. However, irrespective of the data analyses performed, CXCL12γ and IFNγ remained non-differentiable on the 9-CoCRRs array.

In summary, we have demonstrated that a collection of combinatorial surfaces, generated by the self-assembly of only two small and easily synthesized molecules, behave as CRRs and allow the identification of single as well as mixed proteins in solution using SPRi detection. In addition to the straightforward preparation of such devices, the identification of analytes was greatly simplified with analysis using continuous evolution profiles or landscapes. To differentiate HSbps with similar but not identical surface charge topologies, we are currently enhancing the CoCRRs diversity in the arrays by introducing additional BBs with complementary physicochemical properties. We believe that this new approach will contribute to the design of cheaper and more reliable CRR sensor arrays for the rapid implementation of an electronic tongue.

Received: July 6, 2012
Published online: September 11, 2012

Keywords: biosensors · electronic tongue · heparan sulfates · pattern recognition · surface plasmon resonance

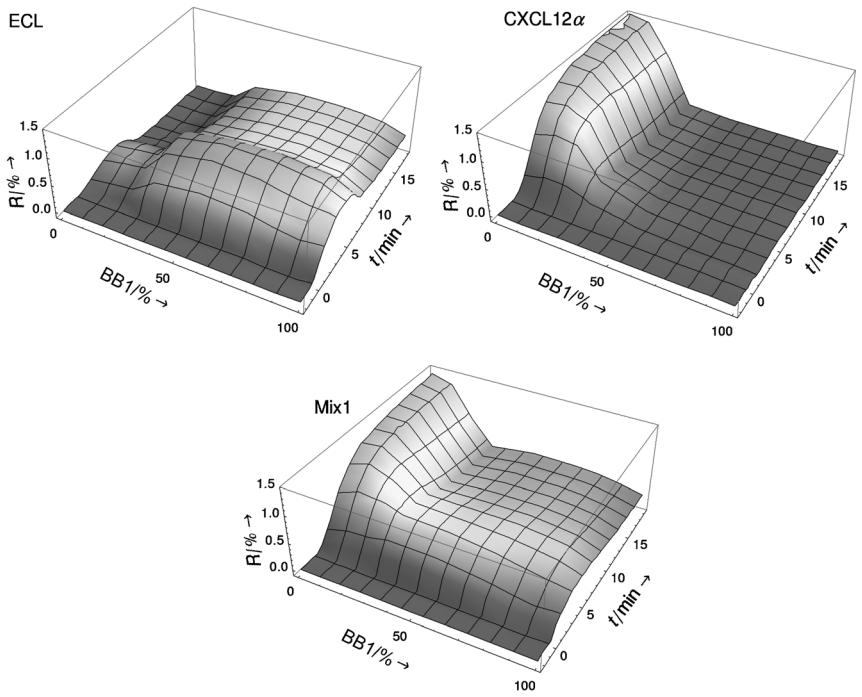

Figure 5. Continuous evolution landscapes (CEL): 3D model of the recognition patterns of ECL, CXCL12α, and Mix1 (ECL + CXCL12α) versus time.

[1] L. D. Bonifacio, G. A. Ozin, A. C. Arsenault, *Small* **2011**, *7*, 3153 – 3157.
[2] A. K. Deisingh, D. C. Stone, M. Thompson, *Int. J. Food Sci. Technol.* **2004**, *39*, 587 – 604.
[3] J. W. Gardner, T. C. Pearce, S. Friel, P. N. Bartlett, N. Blair, *Sens. Actuators B* **1994**, *18*, 240 – 243.
[4] H. Lin, M. Jang, K. S. Suslick, *J. Am. Chem. Soc.* **2011**, *133*, 16786 – 16789.
[5] L. Feng, C. J. Musto, J. W. Kemling, S. H. Lim, W. Zhong, K. S. Suslick, *Anal. Chem.* **2010**, *82*, 9433 – 9440.
[6] S. H. Lim, L. Feng, J. W. Kemling, C. J. Musto, K. S. Suslick, *Nat. Chem.* **2009**, *1*, 562 – 567.
[7] G. Peng, E. Trock, H. Haick, *Nano Lett.* **2008**, *8*, 3631 – 3635.
[8] G. Peng, U. Tisch, O. Adams, M. Hakim, N. Shehada, Y. Y. Broza, S. Billan, R. Abdah-Bortnyak, A. Kuten, H. Haick, *Nat. Nanotechnol.* **2009**, *4*, 669 – 673.

[9] Y. Zilberman, U. Tisch, G. Shuster, W. Pisula, X. Feng, K. Müllen, H. Haick, *Adv. Mater.* **2010**, *22*, 4317 – 4320.
[10] M. Hakim, S. Billan, U. Tisch, G. Peng, I. Dvrokind, O. Marom, R. Abdah-Bortnyak, A. Kuten, H. Haick, *Br. J. Cancer* **2011**, *104*, 1649 – 1655.
[11] J. J. Lavigne, E. V. Anslyn, *Angew. Chem.* **2001**, *113*, 3212 – 3225; *Angew. Chem. Int. Ed.* **2001**, *40*, 3118 – 3130.
[12] D. Margulies, A. D. Hamilton, *Curr. Opin. Chem. Biol.* **2010**, *14*, 705 – 712.
[13] A. T. Wright, E. V. Anslyn, *Chem. Soc. Rev.* **2006**, *35*, 14 – 28.
[14] A. P. Umali, E. V. Anslyn, *Curr. Opin. Chem. Biol.* **2010**, *14*, 685 – 692.
[15] L. Baldini, A. J. Wilson, J. Hong, A. D. Hamilton, *J. Am. Chem. Soc.* **2004**, *126*, 5656 – 5657.
[16] H. C. Zhou, L. Baldini, J. Hong, A. J. Wilson, A. D. Hamilton, *J. Am. Chem. Soc.* **2006**, *128*, 2421 – 2425.
[17] A. T. Wright, M. J. Griffin, Z. L. Zhong, S. C. McCleskey, E. V. Anslyn, J. T. McDevitt, *Angew. Chem.* **2005**, *117*, 6533 – 6536; *Angew. Chem. Int. Ed.* **2005**, *44*, 6375 – 6378.
[18] C. C. You, O. R. Miranda, B. Gider, P. S. Ghosh, I. B. Kim, B. Erdogan, S. A. Krovi, U. H. F. Bunz, V. M. Rotello, *Nat. Nanotechnol.* **2007**, *2*, 318 – 323.
[19] R. L. Phillips, O. R. Miranda, C. C. You, V. M. Rotello, U. H. F. Bunz, *Angew. Chem.* **2008**, *120*, 2628 – 2632; *Angew. Chem. Int. Ed.* **2008**, *47*, 2590 – 2594.
[20] A. Bajaj, O. R. Miranda, I. B. Kim, R. L. Phillips, D. J. Jerry, U. H. F. Bunz, V. M. Rotello, *Proc. Natl. Acad. Sci. USA* **2009**, *106*, 10912 – 10916.
[21] M. De, S. Rana, H. Akpinar, O. R. Miranda, R. R. Arvizo, U. H. F. Bunz, V. M. Rotello, *Nat. Chem.* **2009**, *1*, 461 – 465.
[22] E. Mercey, R. Sadir, E. Maillart, A. Roget, F. Baleux, H. Lortat-Jacob, T. Livache, *Anal. Chem.* **2008**, *80*, 3476 – 3482.
[23] J. Fuchs, J. B. Fiche, A. Buhot, R. Calemczuk, T. Livache, *Biophys. J.* **2010**, *99*, 1886 – 1895.
[24] J. Kreuger, D. Spillmann, J. P. Li, U. Lindahl, *J. Cell Biol.* **2006**, *174*, 323 – 327.
[25] M. Petitou, C. A. A. van Boeckel, *Angew. Chem.* **2004**, *116*, 3180 – 3196; *Angew. Chem. Int. Ed.* **2004**, *43*, 3118 – 3133.
[26] A. Imberty, H. Lortat-Jacob, S. Perez, *Carbohydr. Res.* **2007**, *342*, 430 – 439.
[27] H. Lortat-Jacob, A. Grosdidier, A. Imberty, *Proc. Natl. Acad. Sci. USA* **2002**, *99*, 1229 – 1234.
[28] M. P. Dubois, C. Gondran, O. Renaudet, P. Dumy, H. Driguez, S. Fort, S. Cosnier, *Chem. Commun.* **2005**, 4318 – 4320.
[29] C. Laguri, R. Sadir, P. Rueda, F. Baleux, P. Gans, F. Arenzana-Seisdedos, H. Lortat-Jacob, *PLoS One* **2007**, *2*, e1110.
[30] S. Sarrazin, D. Bonnaffe, A. Lubineau, H. Lortat-Jacob, *J. Biol. Chem.* **2005**, *280*, 37558 – 37564.
[31] K. Turton, R. Natesh, N. Thiyagarajan, J. A. Chaddock, K. R. Acharya, *Glycobiology* **2004**, *14*, 923 – 929.
[32] M. Reynolds, M. Marradi, A. Imberty, S. Penadés, S. Pérez, *Chem. Eur. J.* **2012**, *18*, 4264 – 4273.
[33] S. J. Stranick, S. V. Atre, A. N. Parikh, M. C. Wood, D. L. Allara, N. Winograd, P. S. Weiss, *Nanotechnology* **1996**, *7*, 438 – 442.
[34] H. Lortat-Jacob, *Curr. Opin. Struct. Biol.* **2009**, *19*, 543 – 548.
[35] H. Lortat-Jacob, J. E. Turnbull, J. A. Grimaud, *Biochem. J.* **1995**, *310*, 497 – 505.
[36] D. Bonnaffé, *C. R. Chim.* **2011**, *14*, 59 – 73.

